

This article was downloaded by: [CDL Journals Account]

On: 11 January 2011

Access details: Access Details: [subscription number 922973516]

Publisher Taylor & Francis

Informa Ltd Registered in England and Wales Registered Number: 1072954 Registered office: Mortimer House, 37-41 Mortimer Street, London W1T 3JH, UK



Synchrotron Radiation News

Publication details, including instructions for authors and subscription information:

<http://www.informaworld.com/smpp/title~content=t716100695>

Infrared Spectromicroscopy: Probing Live Cellular Responses to Environmental Changes

Hoi-Ying N. Holman^a; Zhao Hao^a; Michael C. Martin^b; Hans A. Bechtel^b

^a Earth Sciences Division, Lawrence Berkeley National Laboratory, Berkeley, CA, USA ^b Advanced Light Source Division, Lawrence Berkeley National Laboratory, Berkeley, CA, USA

Online publication date: 09 October 2010

To cite this Article Holman, Hoi-Ying N. , Hao, Zhao , Martin, Michael C. and Bechtel, Hans A.(2010) 'Infrared Spectromicroscopy: Probing Live Cellular Responses to Environmental Changes', Synchrotron Radiation News, 23: 5, 12 – 19

To link to this Article: DOI: 10.1080/08940886.2010.516737

URL: <http://dx.doi.org/10.1080/08940886.2010.516737>

PLEASE SCROLL DOWN FOR ARTICLE

Full terms and conditions of use: <http://www.informaworld.com/terms-and-conditions-of-access.pdf>

This article may be used for research, teaching and private study purposes. Any substantial or systematic reproduction, re-distribution, re-selling, loan or sub-licensing, systematic supply or distribution in any form to anyone is expressly forbidden.

The publisher does not give any warranty express or implied or make any representation that the contents will be complete or accurate or up to date. The accuracy of any instructions, formulae and drug doses should be independently verified with primary sources. The publisher shall not be liable for any loss, actions, claims, proceedings, demand or costs or damages whatsoever or howsoever caused arising directly or indirectly in connection with or arising out of the use of this material.

Infrared Spectromicroscopy: Probing Live Cellular Responses to Environmental Changes

HOI-YING N. HOLMAN¹, ZHAO HAO¹, MICHAEL C. MARTIN², AND HANS A. BECHTEL²

¹Earth Sciences Division, Lawrence Berkeley National Laboratory, Berkeley, CA, USA

²Advanced Light Source Division, Lawrence Berkeley National Laboratory, Berkeley, CA, USA

The recent advent of gene sequencing and high-throughput functional genomic approaches has led to a paradigm shift in studying microbial responses to environmental changes—from a reductionist approach of studying the structure and function of individual cellular parts to global investigations of increasingly complex systems of molecules and their interactions. While gene sequencing and high-throughput functional genomic approaches have already allowed researchers to focus on a genome-based understanding of both the individual cellular parts and the biochemical networks, we now need new capabilities that will enable investigation of biochemical processes as a whole in living cells. Today, much of our understanding has come from biochemistry experiments that are averaged over large populations of cells. These approaches have clarified many detailed mechanisms, but they are not sufficient to reveal the differences that exist even within a genetically homogeneous population. For example, recent single-molecule imaging studies of living cells have revealed that the cellular reactions that occur in complex networks of regulatory and metabolic processes during adaptive responses may exhibit both spatial and temporal separation within a population or a community. This heterogeneity, which can be of ecological significance, clearly cannot be evaluated in experiments that are averaged over large populations. The challenge is to identify those cells of ecological importance within a large population and track their biochemical reactions in situ in real time. In this article, we first describe how we can help to meet this challenge by combining a classical infrared approach (used to study cells and living tissues for over six decades) with a brilliant synchrotron and an appropriate microfluidic platform, followed by three application examples.

Infrared Spectroscopy

Infrared spectroscopy in the mid-infrared region (~ 2.5 to ~ 15.5 μm wavelength, or ~ 4000 to ~ 650 wavenumber in cm^{-1}) is a powerful and nondestructive analytical technique that provides label-free, fingerprint-like spectra originating from the characteristic vibrational frequencies of various chemical bonds and functional groups [1]. Changes in hydrogen bond lengths of as little as 0.01 \AA or in bond angles of as little as 1° can be clearly differentiated in a vibrational spectrum [2]. This specificity and sensitivity makes infrared spectroscopy an excellent tool for studying the structure and function of biological macromolecules. The introduction of fast Fourier transform infrared (FTIR) spectromicroscopy (also called

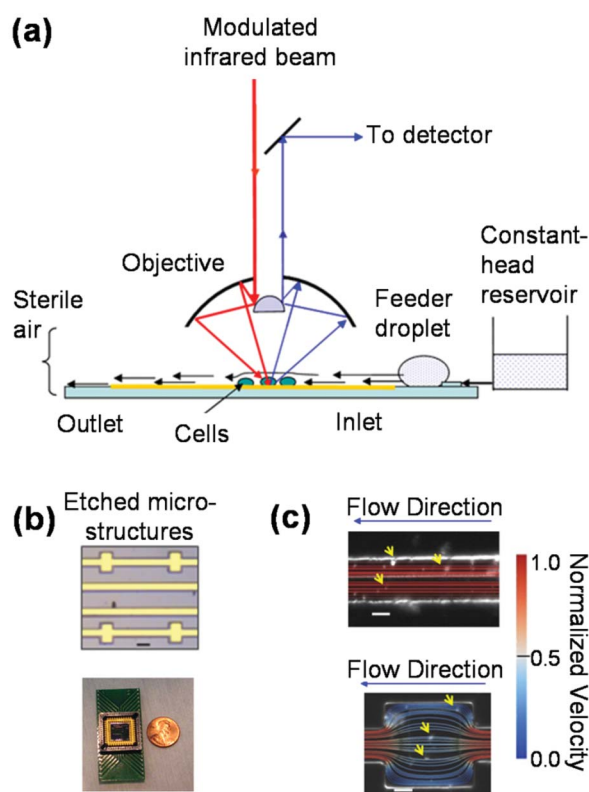


Figure 1: Microfluidic platform to minimize water absorption. (a) Microfluidic SR-FTIR microscopy platform schematic. (b) Plane view depiction of a chip with several parallel etched microstructures for simultaneous experiments. (c) Flow maps of the microstructures, simulated from experimentally measured paths of near-neutral density polystyrene beads (yellow arrows) and superimposed on a snapshot image; top, flow in a microchannel; bottom, flow in a microwell. Scale bars = 10 μm . Velocity = ~ 60 $\mu\text{m/s}$ (adapted from Ref. 28)

microspectroscopy) improved speed and sensitivity. Ultimately, both spatial resolution and detection sensitivity can be significantly improved by replacing the thermal emission source in the conventional FTIR spectromicroscope with a bright synchrotron infrared source [3,4].



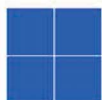
CCD X-Ray Detectors

Typical delivery is 14 - 16 weeks ARO.
Contact the ADSC sales office for a
pricing discount on a multiple detector
system purchase. Installation and
applicable training are included.



Technical Summary (typical):

	Quantum 315 r	Quantum 210 r
Detector Type:	3 x 3 Array	2 x 2 Array
Active Area:	315mm x 315mm	210mm x 210mm
Number of Pixels:	6140 x 6140; 37.75M	4096 x 4096; 16.8M
Pixel Size at Detector Surface:	51 x 51 microns	51 x 51 microns
Phosphor (optimized):	1 Angstrom X-rays	1 Angstrom X-rays
Spatial Resolution FWHM:	90 microns; 1.76 pixels	90 microns; 1.76 pixels
Taper Ratio:	3.7 : 1	3.7 : 1
Optical Coupling (CCD to Taper):	Hard Epoxy Bond	Hard Epoxy Bond
CCD Type:	Atmel THX 7899	Atmel THX 7899
CCD Pixel Size:	14 x 14 microns	14 x 14 microns
Operating Temperature:	-45 degrees Celsius	-45 degrees Celsius
Cooling Type:	Thermoelectric	Thermoelectric
Dark Current:	0.015 e/pixel/second	0.015 e/pixel/second
Controller Electronics:	ADSC Custom	ADSC Custom
Readout Times:		
Full Resolution:	0.90 seconds	0.90 seconds
2x2 Hardware Binned:	0.25 seconds	0.25 seconds
2x2 Software Binned:	0.90 seconds	0.90 seconds
Readout Noise		
Full Resolution:	11 electrons	11 electrons
2x2 Hardware Binned:	11.5 electrons	11.5 electrons
2x2 Software Binned:	2 x 11 electrons	2 x 11 electrons
Dynamic Range		
Full Resolution:	18,100	18,100
2x2 Hardware Binned:	22,600	22,600
2x2 Software Binned:	36,300	36,300
Full Well Depth (low noise MPP mode)		
Full Resolution:	200,000 electrons	200,000 electrons
2x2 Hardware Binned:	260,000 electrons	260,000 electrons
2x2 Software Binned:	800,000 electrons	800,000 electrons
DQE:	> 80%	> 80%
Dimensions:	880mm x 450mm x 460mm	805mm x 346mm x 316mm
Weight:	133 Kgs	58 Kgs



ADSC

Area Detector Systems Corporation

12550 Stowe Drive, Poway, California 92064 USA

Sales: (858) 486-0618 Fax: (858) 486-0722 email: sales@adsc-xray.com

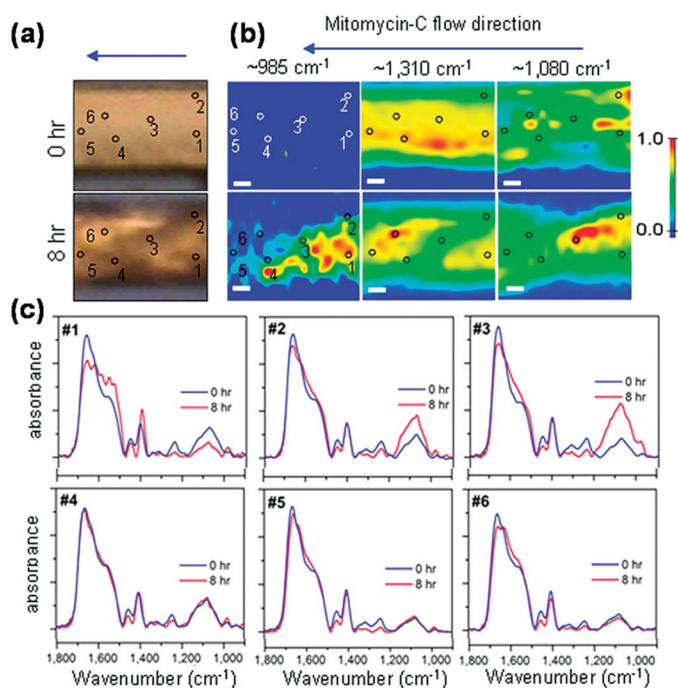


Figure 2: Interactions of antibiotics with *E. coli*. (a) Optical images of day-old *E. coli* biofilm before (0 hr) and during (8 hr) MMC exposure. (b) SR-FTIR chemical image plots of the intensity, before (upper panels) and during (lower panels) MMC exposure, at $\sim 985\text{ cm}^{-1}$ (DNA-MMC adducts), $\sim 1310\text{ cm}^{-1}$ (protein amide III), and $\sim 1080\text{ cm}^{-1}$ (polysaccharides). Arrows indicate MMC stream direction. Scale bars: $10\text{ }\mu\text{m}$. (c) Preprocessed SR-FTIR spectra at selected locations before (blue spectra) and during (red spectra) MMC exposure (adapted from Ref. 15)

The Brilliance of Synchrotron Radiation

Synchrotron radiation (SR) is 100–1000 times brighter than a conventional thermal infrared source. When coupled to an infrared microscope, the greater brightness means that the photons can be focused to a diffraction-limited spot dependent on the numerical aperture (NA) of the microscope objective and the wavelength (λ) of light. Typical infrared microscopes use Schwarzschild objectives with NA in the range of 0.4 to 0.7, and spot sizes (and hence spatial resolutions) of 0.5λ to 1.2λ are achievable [3,5].

It is important to consider the size of the individual cells relative to the size of the infrared beam during the design of biological investigations. In the mid-infrared region, these 0.5λ to 1.2λ (i.e., ~ 2 to $\sim 10\text{ }\mu\text{m}$) diffraction-limited spot sizes are smaller than eukaryote cells, bigger than most of the prokaryotes or archaea, and are comparable to a small cluster of prokaryote or archaea cells. Unlike with a thermal source that must use apertures to achieve micrometer spatial resolution, with a synchrotron source there is no loss in signal-to-noise ratio (SNR). Although many more infrared photons are focused on the biological sample when using a synchrotron source, the low photon energy and low peak powers (relative to the alternative infrared laser sources) of $< 50\text{ mW}$ have shown no detectable effects on living cells [6].

Improved spatial resolution is of great benefit to measurements involving heterogeneous samples. The accuracy with which a given feature is measured is greatly increased because the measurement is taken only from the area of interest [4]. The improvement in SNR and time resolution of SR-FTIR is demonstrated by comparing spectra from a single cell as measured with a synchrotron and a conventional thermal source. The collection time using the synchrotron source was only 16 seconds (32 scans), whereas the thermal source took 500 seconds (1000 scans). Even after extensive averaging, the quality of the thermal source measurement is not sufficient to reveal the fine molecular features within the vibrational spectrum.

The high SR-IR brightness coupled with its noninvasive nature has already made a significant impact in the fields of biomedicine [7], environmental ecology, and geochemistry [8]. In an early study from our group, time-lapse SR-FTIR reflectance measurements showed the mechanism by which a small subset of microbes on a basalt rock specimen survived exposure to a high concentration of toxic chromium(VI) when most of the surrounding microbial cells were killed [9]. Although geological materials inherently have very rough surfaces, the small spot size of the SR infrared source allowed us to measure a small region with a handful of microorganisms, revealing that they were reducing chromium(VI) to chromium(III). This capability also yielded new insights into how the soil bacteria *Mycobacterium* sp. JLS solubilize large recalcitrant organic pollutants like polycyclic aromatic hydrocarbons and metabolize them into biomass [10]. These insights into dynamic microbial processes in simulated geological environments have been included in the design of environmental clean-up strategies.

A “Just Right” Microfluidic Platform

Water presents one of the primary challenges of using infrared spectroscopy in studying living cells, even with a bright synchrotron source. Water strongly absorbs mid-infrared light, and even the absorption of a thin layer of water can completely dominate the spectrum. However, water is necessary for life and is the most common ingredient ($> 70\%$) in living cells. The trick is to get the optical thickness of the water just right: enough to support life but not so much that it masks the molecular signatures of interest. Typically less than ten micrometers of bulk water is preferred if one wants to exploit the molecular information across the full mid-infrared spectral range.

A traditional approach to minimizing water absorption during living-cell experiments is attenuated total reflectance (ATR) FTIR equipped with a flow chamber. In ATR-FTIR, the IR beam is internally reflected off a high-index crystal (e.g. diamond or germanium) and the attenuation of the beam is measured and analyzed [11]. For living-cell experiments, cells are cultured on ATR crystals in a specially designed flow chamber that can carefully control the culturing/experimental conditions (pH, temperature, ionic strength, flow shear stress, and delivery of materials such as nutrients and drugs) for hours [12–14]. The attenuated field formed at the cell/ATR crystal interface has a typical penetration depth of less than one micrometer, thereby reducing the optical path length in water. However, this small penetration depth, while important in reducing the path

length through water, prevents the ATR-FTIR technique from examining chemical and biological processes in cells of biological systems with an extensive extracellular matrix. Another important consideration is the effect of growing the cells on the ATR crystal, which may affect extracellular matrix properties that are important in cellular phenotype.

We used a more straightforward microfluidic approach instead [15]. Figure 1 shows an early version of our open-channel microfluidic device. It was fabricated on a silicon chip using deep reactive ion etching to create hydrophilic microstructures 10–15 μm deep and at least 40 μm wide. A continuous thin-film ($<10\text{ }\mu\text{m}$) laminar flow is maintained by balancing the hydrostatic pressure in a microliter-size feeder droplet at the microchannel inlet with the capillary forces present at the outlet. Mid-infrared photons emitted from the synchrotron are focused onto the targeted areas within the microstructures, and SR-FTIR measurements are made by the transfection or transmission modes. To image the biochemical properties and the distribution of bacterial activity across a biofilm, it is raster scanned with equal micrometer-sized steps, collecting a full SR-FTIR spectrum at each position. The ability of the platform to provide a sustainable environment for SR-FTIR measurements of living bacteria has been confirmed by using the reporter bacterium *E. coli* XL1-blue.

Several other groups have reported uncomplicated flow chamber techniques [16–18] that place living cells between two parallel infrared

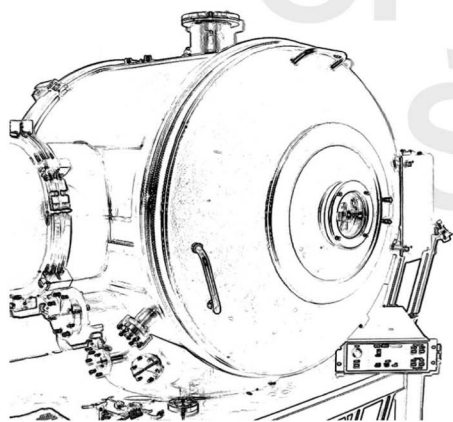
transparent windows (e.g., CaF_2) separated by a spacer of minimum thickness ($<12\text{ }\mu\text{m}$). Although effective in its simplicity, we found that the spectra from closed-chamber or closed-channel devices are often marred by interference fringes that probably arise from multiple reflections from the parallel surfaces. In our device, the sloping free interface between water and air has allowed us to completely eliminate the interference fringes during FTIR measurements.

Example 1: Understanding Bacteria–Antibiotic Interactions in a Biofilm

A bacterial biofilm is a population of cells growing on a surface and enclosed in a self-produced polymeric matrix in aqueous environments. Bacteria within a biofilm can become up to 1000 times more resistant to antibiotics than those of free-floating bacteria of the same species [19], yet only about 1% of their genes shows differential expression between these two types of population [20].

Figure 2 shows an example of using open-channel microfluidics with SR-FTIR spectromicroscopy to study why some *E. coli* in biofilms are not killed by the antimicrobial agent mitomycin-C (MMC) [15]. MMC is activated only after it has entered a cell, where it is then reduced to a hydroquinone form that covalently cross-links to guanine residues in DNA to form DNA-MMC adducts [21]. The presence of DNA-MMC adduct signals at $\sim 986\text{ cm}^{-1}$ reflects cellular uptake and the action of

x-ray mirrors for synchrotron applications



mirror coating system

Middle Barton, Whittingham, Alnwick, Northumberland, NE66 4SU, UK
Tel: +44 1665 574440 Fax: +44 1665 574446 sales@crystal-scientific.com

NEW PRODUCTS FROM CRYSTAL SCIENTIFIC

XSM™ - the range of x-ray synchrotron mirrors, in cooled and un-cooled versions.

KBfocus™ - an advanced Kirkpatrick-Baez pair product for focused x-ray applications.

These products build on our range of diffraction optics in use at synchrotrons worldwide.

Precision manufacture and characterisation expertise, from the specialist supplier of x-ray optics for synchrotron applications.

www.crystal-scientific.com

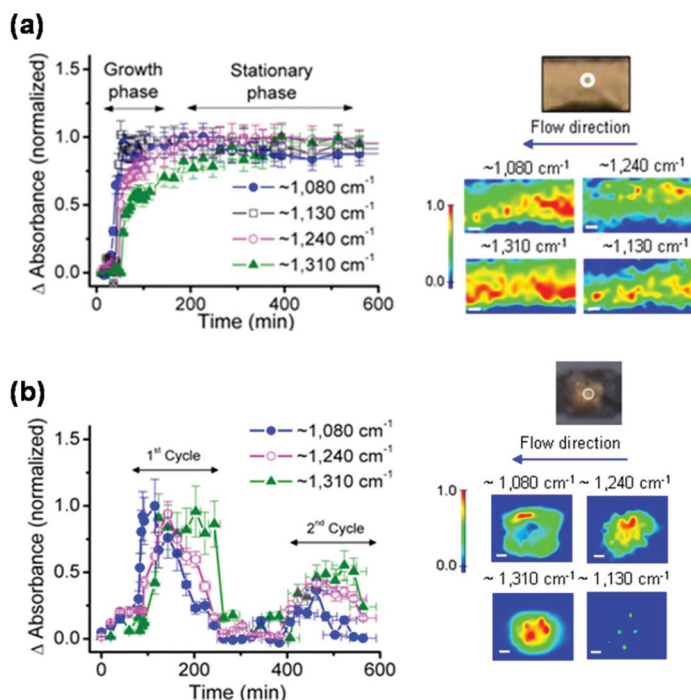


Figure 3: Biofilm dynamics. SR-FTIR time course analyses and chemical images of biofilms (a) in a microchannel and (b) in a microwell (as shown by four molecular markers at $\sim 1080\text{ cm}^{-1}$ (polysaccharides), $\sim 1130\text{ cm}^{-1}$ (glycocalyx), $\sim 1240\text{ cm}^{-1}$ (DNA/RNA polysaccharides), and $\sim 1310\text{ cm}^{-1}$ (protein amide III)). Unlike the microchannel data, where signal intensity of key biomolecules appeared to approach an asymptotic state, the microwell SR-FTIR data were cyclic (cell growth and release). The chemical image plots obtained after the second cycle show locally higher signal intensities of protein amide III ($\sim 1310\text{ cm}^{-1}$) and DNA/RNA polysaccharides ($\sim 1240\text{ cm}^{-1}$) near the microwell center, whereas the polysaccharide matrix accumulated near the microwell edge. There is little spectroscopic evidence of glycocalyx ($\sim 1130\text{ cm}^{-1}$) to facilitate strong adherence to the microwell substrate. Scale bars = $10\text{ }\mu\text{m}$ (adapted from Ref. 15).

MMC [15]. Figure 2b shows chemical images before and after the introduction of MMC into the microfluidic system. Despite an uninterrupted supply of MMC-laden water, the SR-FTIR image plot shows that MMC uptake is highly localized. DNA-MMC adduct signals are especially strong in areas that were either closer to the MMC source (locations 1 and 2 in the figure) or in areas formerly rich in protein amide III ($\sim 1310\text{ cm}^{-1}$). In areas with little DNA-MMC adduct, the protein amide III signal increased with MMC exposure. Shown in Figure 2c are analyses of vector-normalized SR-FTIR spectra (over the $900\text{--}1800\text{ cm}^{-1}$ region) at different locations; they also indicate localized small (~ 10 to $\sim 20\text{ }\mu\text{m}$) changes in biochemical contents consequent to MMC exposure. We speculate that the localization of MMC may be caused by flow heterogeneities inside the biofilms, perhaps related to internal flow diversions around regions with higher protein amide III signal. The heterogeneous spectral

features and behavior, however, may also reflect localized cellular diversification processes in response to MMC toxicity, such as metabolic modification and/or migration to more favorable living areas.

Example 2: Revealing Biofilm Dynamics

Our group also used the open-channel SR-FTIR platform to improve understanding of the growth and development of bacteria on surfaces. Many microbial processes important in pathogenesis and ecology are initiated in confined microscopic spaces, and recent reports indicate that the colonizing bacterial cells actively seek out confined spaces where biofilm initiation, formation, and evolution can be influenced by fluid dynamics, nutrient supplies, or waste removal.

We compared biofilm formation in microchannels (with higher rates of nutrient supplies and waste product removal) to that in microwells (with lower rates of nutrient supplies and waste removal) (see Figure 3) [15]. For microchannels, four different markers of biofilm formation increase asymptotically: polysaccharide ($\sim 1080\text{ cm}^{-1}$), glycocalyx ($\sim 1130\text{ cm}^{-1}$), DNA/RNA ($\sim 1240\text{ cm}^{-1}$), and protein amide III ($\sim 1310\text{ cm}^{-1}$) (see Figure 3a). This result provides chemical evidence that biofilm formation proceeds via multiple convergent genetic pathways. The abundance of glycocalyx carbohydrates in sites with large biofilm growth confirms the belief that glycocalyx synthesis is crucial to the formation of bacterial biofilms [22]. In contrast, biofilm formation in microwells exhibits cyclic growth patterns as indicated by the sequential rise and fall of the different biomolecule signals (see Figure 3b). The lack of spectroscopic evidence of glycocalyx suggests that biofilm attachment was weaker in the microwell. It was discovered most recently that some bacteria can produce a factor (mixtures of D-amino acids) that could prevent biofilm formation and cause the breakdown of existing biofilms [23].

Example 3: Delineating Genome-Based Chemistry of Oxygen Stress and Adaptive Response

One of our earlier applications was to study how descendants of some of the oldest bacteria can survive the oxygen stress of modern Earth. Microbes such as the ubiquitous sulfate-reducing bacteria (SRB) are the oldest (> 3.5 billion years) and smallest (about $1/8000$ th the volume of a human cell) living organisms on Earth. It is believed that their high surface-to-volume ratio and strong selection pressure have yielded preparations to cope with environmental fluctuation. Genome sequencing shows that some SRB descendants have acquired the genetic “blueprints” to survive transiently an oxygenated atmosphere. This includes the potential capabilities to reduce (di)oxygen and cope with the subsequent toxic reactive oxygen species (ROS) in the modern atmosphere, such as superoxide anion radicals, peroxides, and hydroxyl radicals.

In the case of our model SRB, *Desulfovibrio vulgaris* Hildenborough, only a small number of cells in a population can survive transient exposure to atmospheric oxygen (see Figure 4a). These few survivors often exist individually or in small groups of several cells to form localized microscopic communities. They must be interrogated without spectroscopic influence from neighboring cells that are dying. We also know

that the time scales of the oxygen adaptive response processes can potentially range from minutes to hours [24]. To avoid long data acquisition times and thus capture the response dynamics at shorter time scales, a brilliant infrared source providing high SNR is required.

Our previous experience showed that only cells entering the early stationary phase of the cell cycle and accumulating an internal reserve of polyglucose and elemental sulfur are likely to survive transient air exposure [25]. The FTIR spectra of polyglucose-accumulated *D. vulgaris* (see Figures 4b and 4c) show the distinct spectral features of the non-glycosidic polyglucose vibration ($\nu\text{C-OH}$) band between 1055 and 1045 cm^{-1} and the glycosidic linkage vibration ($\nu\text{C-O-C}$) at $\sim 1175 \text{ cm}^{-1}$ (see Figure 4b). This spectral information is used to look for potential survivors in a thin layer of *D. vulgaris* clones that are maintained in an oxygen-free moist atmosphere inside the microscope-stage environmental chamber. By rastering the diffraction-limited synchrotron infrared beam across the thin film, one can identify spots where the spectrum exhibits features similar to the typical spectrum of polyglucose-bearing living *D. vulgaris*.

The graph in Figure 5a is an overview of the striking molecular changes in *D. vulgaris* survivors during their exposure to atmospheric oxygen. The trends seen in Figures 5b and 5c, which were derived from spectrally integrated absorption intensities of polyglucose and water bands [25], reveal an unanticipated multiphasic pattern. These two molecules are of immediate interest because the reduction of di-oxygen to water through aerobic respiration of internal polyglucose reserves was previously believed to be the primary step in air-tolerant SRB. Comparing trends in these two figures shows that from 0 to ~ 50 minutes there is a substantial decrease in the polyglucose band intensity but little change in the water band intensity. After ~ 50 minutes, the water band intensity increases abruptly while the rate of polyglucose disappearance continues unabated until slowing down distinctly later (after ~ 100 minutes).

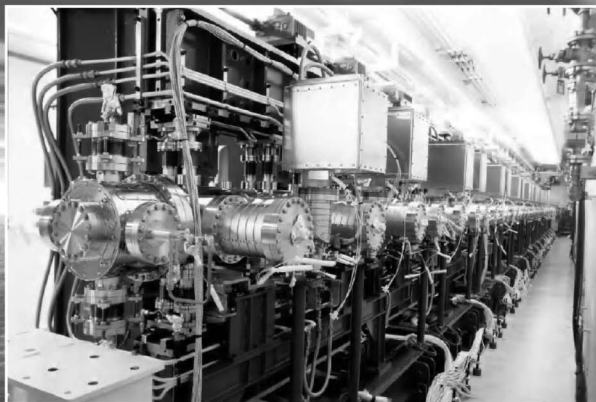
Figure 5d is a two-dimensional time-frequency contour plot of the time-difference spectra (negative values are shown in dark blue), with difference spectrum snapshots beneath (see Figure 5e). The contour map reveals the remarkable changing absorption features from νOH as



HITACHI

Advanced Undulator !

— Design & Manufacturing —



Courtesy of Spring-8



Courtesy of KEK



Hitachi Metals, Ltd.

<http://www.hitachi-metals.co.jp/e/index.html>

Hitachi Metals America, Ltd. Tel +1-224-366-8221
Hitachi Metals Europe GmbH Tel +49-7152-939-751
NEOMAX ENGINEERING Co., Ltd. Tel +81-3-5765-4250

E-mail neo.horimoto@hitmet.com
E-mail tkamiyama@hitachi-metals-europe.com
E-mail Sachio_Hirano@hitachi-metals.co.jp

NEOMAX

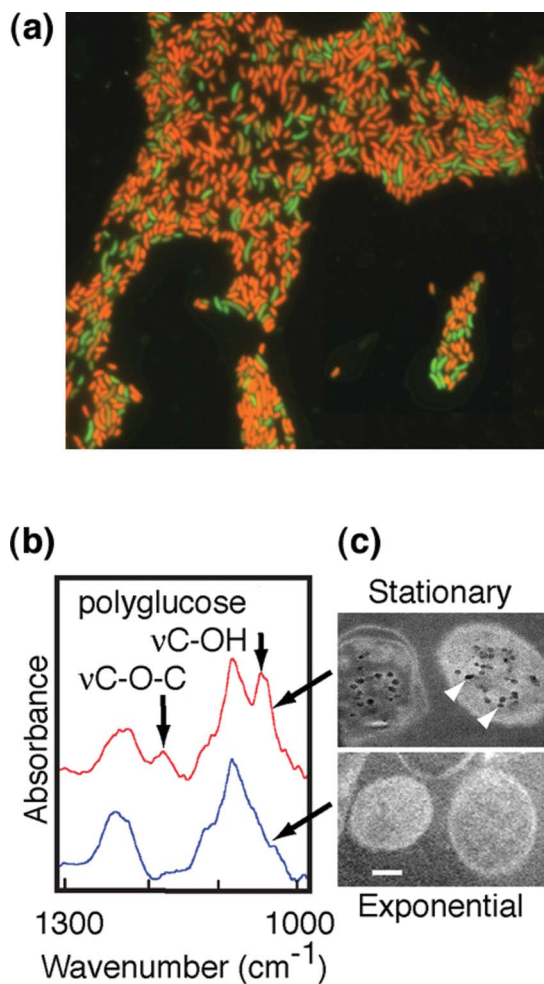


Figure 4: Survivor SRB. (a) Viability of SRB after exposure to moist air for eight hours. Live (green) and dead (red) were assessed using reagents in LIVE/DEAD BacLight Bacterial Viability kit. (b) Typical infrared absorption spectra of stationary-phase (red) and exponential-phase (blue) *D. vulgaris*. (c) Transmission electron microscopy images of thin sections post-stained by the periodic acid thiosemicarbazide-osmium (PATO) method show intracellular polyglucose granules in stationary-phase but not exponential-phase *D. vulgaris* (adapted from Ref. 25).

a function of time, which reflects a cascade of chemical reactions (see Figure 5f) that sheds light on genetically controlled pathways [25].

The mechanisms by which SRB survive transient exposure to atmospheric oxygen have been controversial, partly because of the approach of averaging over a large population. Our SR-FTIR technique provides the first direct molecular observation of the reduction of di-oxygen to water by a small number of SRB through aerobic respiration of internal polyglucose reserves as one crucial step and identifies the transient chemical reactions that allow the survivor subpopulation to adapt to extreme changes in its environment.

Prospects

The next step in the development of infrared spectromicroscopy is the improvement of imaging speed. This is required for studying multiple sub-populations simultaneously within an isogenetic population and for developing a fundamental understanding of population-level diversity. Currently, even with the huge improvements in SNR from a synchrotron source, mapping large areas at high spatial resolution with the raster scanning technique can be extraordinarily time intensive. For example, imaging a $100 \times 100 \mu\text{m}$ area with a $3\text{-}\mu\text{m}$ step size can take nearly 20 minutes. Using longer average measurement times to improve the SNR can easily increase the acquisition time to hours or days! Focal plane array (FPA) technology has increased the speed of image acquisition by multiplexing the acquisition of data, but low SNRs have limited their applicability. One solution is to couple these new detectors with high-brightness of synchrotron radiation [26]. Presently, many of the thirty-some synchrotron infrared facilities worldwide are investigating this prospect. The InfraRed ENvironmental Imaging

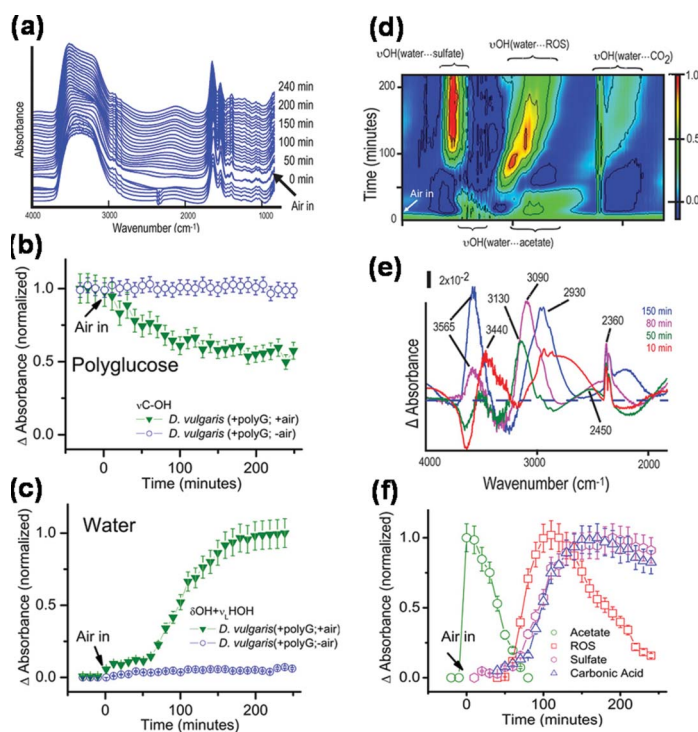


Figure 5: Oxidative stress and adaptation. (a) Typical real-time SR-FTIR spectra of *D. vulgaris* during the transition from an anaerobic to aerobic environment. Since all spectra are derived using air as a reference, the abrupt change in the spectral feature at $\sim 2348 \text{ cm}^{-1}$ is associated with the presence of atmospheric CO_2 . Typical time-course of infrared intensity (normalized by the maximum value) of (b) polyglucose content and (c) water. (d) Time versus frequency contour plot of SR-FTIR time-difference spectra in the hydride-OH dominated stretch region. (e) Snapshots of time-difference spectra for selected different time points. The dashed line marks zero difference absorbance. (f) Typical time-course of infrared intensity (normalized by the maximum value) of H-bonded species (adapted from Ref. 25).

(IRENI) Facility at the Synchrotron Radiation Center (SRC) at the University of Wisconsin-Madison is the first FPA-based SR-FTIR system available to users (www.src.wisc.edu/ireni/).

Another direction is to integrate high-density microfluidic chips with plumbing networks [27]. This advance will enable the automatic and precise manipulation of fluids to provide accurate “on-demand” conditions to study the chemistry of living cells. This will permit investigations of many important cellular systems in aqueous environments over long time periods, including harmful processes like chronic bacterial infections or beneficial processes like energy production by microbes.

Acknowledgments

This work was supported by the U.S. Department of Energy Office of Biological and Environmental Research's Structural Biology Program through contracts DE-AC02-05CH11231, and KP1501021 with Lawrence Berkeley National Laboratory. The Advanced Light Source is supported by the Director, Office of Science, Office of Basic Energy Sciences, of the U.S. Department of Energy under contract DE-AC02-05CH11231. The viability micrograph was prepared by Dominique C. Joyner.

References


1. F.S. Parker, *Applications of Infrared, Raman, and Resonance Raman Spectroscopy in Biochemistry*, Plenum Press: New York & London (1983).
2. G.A. Jeffrey, *An Introduction to Hydrogen Bonding*, Oxford University Press: New York (1997).
3. G.L. Carr et al., *Rev. Sci. Instrum.* **66**, 1490 (1995).
4. P. Dumas et al., *J. Trends Biotechnol.* **25**, 40 (2007).
5. E. Levenson et al., *Infrared Phys. Tech.* **51**, 413 (2008).
6. H.Y.N. Holman et al., *J. Biomed. Opt.* **7**, 417 (2002).
7. L.M. Miller, in *Infrared and Raman Spectroscopic Imaging*, 510, R. Salzer and H.W. Siesler, eds., Wiley-VCH: Weinheim (2009).
8. H.Y.N. Holman and M.C. Martin, in *Advances in Agronomy*, **90**, 79, D. Sparks, ed., Elsevier: New York (2006).
9. H.Y.N. Holman et al., *Geomicrobiol. J.* **16**, 307 (1999).
10. H.Y.N. Holman et al., *Environ. Sci. Technol.* **36**, 1276 (2002).
11. R. Iwamoto and K. Ohta, *Appl. Spectrosc.* **38**, 359 (1984).
12. T.B. Hutson et al., *Anal. Biochem.* **174**, 415 (1988).
13. P.A. Suci et al., *Biomaterials* **19**, 327 (1998).
14. M.K. Kuimova et al., *Appl. Spectrosc.* **63**, 164 (2009).
15. H.Y.N. Holman et al., *Analytical Chemistry* **81**, 8564 (2009).
16. M.J. Nasse et al., *Appl. Spectrosc.* **63**, 1181 (2009).
17. M.J. Tobin et al., *Vib. Spectrosc.* **53**, 34 (2010).
18. G. Birarda et al., *Microelectronic Engineering* **87**, 806 (2010).
19. P.S. Stewart et al., *Nat. Rev. Microbiol.* **6**, 199 (2008).
20. M. Whiteley et al., *Nature* **413**, 860 (2001).
21. J. Portugal et al., *Biochemical Journal* **306**, 185 (1995).
22. J.W. Costerton et al., *Annual Review of Microbiology* **35**, 299 (1981).
23. I. Kolodkin-Gal et al., *Science* **328**, 627 (2010).
24. A. Mukhopadhyay et al., *J. Bacteriol.* **189**, 5996 (2007).
25. H.Y.N. Holman et al., *Proc. Nat. Acad. Sci. USA* **106**, 12599 (2009).
26. C. Petibois et al., *Journal of Synchrotron Radiation* **17**, 1 (2010).
27. T. Thorsen et al., *Science* **298**, 580 (2002).
28. H.-Y. N. Holman et al., *Analytical Chem.*, in press (2010).

Beamline engineering excellence

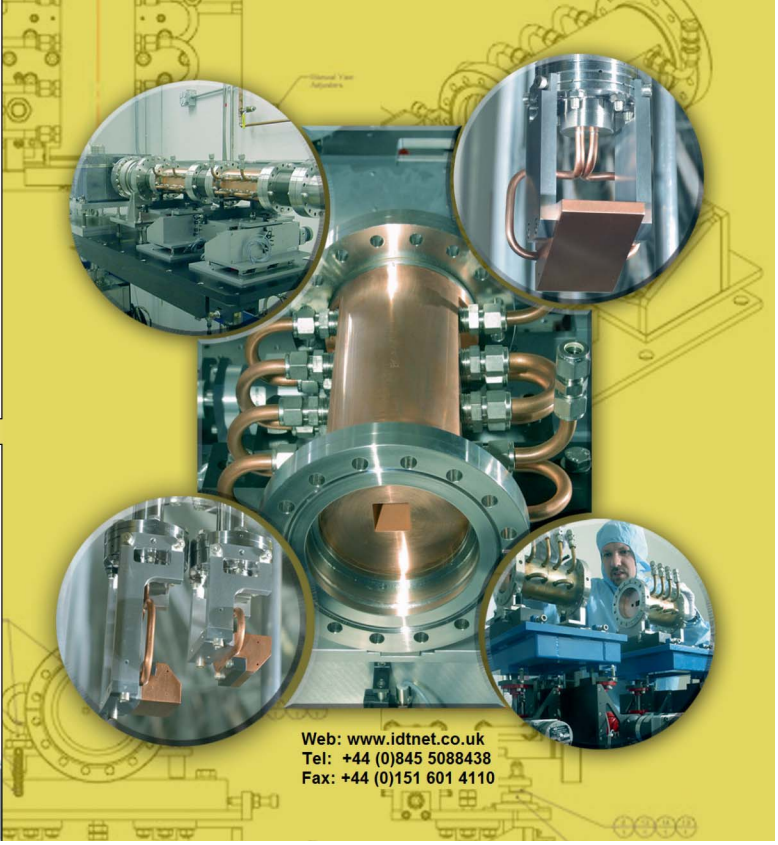
Complete beamlines & custom engineered systems

MONOCHROMATORS
KB MIRROR SYSTEMS

HIGH HEAT LOAD APERTURES
BEAMLINE COMPONENTS
DIAGNOSTICS
EXPERIMENTAL EQUIPMENT
OPTICAL ENGINEERING
COMPREHENSIVE TESTING
INTEGRATED EPICS SOFTWARE



instrument design technology
beamline engineering excellence



Web: www.idtnet.co.uk
 Tel: +44 (0)845 5088438
 Fax: +44 (0)151 601 4110